

Key Points:

- *Pinus ponderosa* in the North American Monsoon region switched from using snowmelt water during early-summer to monsoon rain during late-summer
- During a low snowpack year, trees used less monsoon rain, suggesting that antecedent moisture from snowpack influences summer rain uptake
- Thus, consideration of both antecedent and current soil moisture is required to fully understand how these montane trees in semi-arid ecosystems use different water sources

Supporting Information:

Supporting Information may be found in the online version of this article.

Correspondence to:

K. Bailey,
kinziebailey@arizona.edu

Citation:

Bailey, K., Szejner, P., Strange, B., Monson, R. K., & Hu, J. (2023). The influence of winter snowpack on the use of summer rains in montane pine forests across the southwest U.S.. *Journal of Geophysical Research: Biogeosciences*, 128, e2023JG007494. <https://doi.org/10.1029/2023JG007494>

Received 24 MAR 2023
Accepted 17 AUG 2023

Author Contributions:

Conceptualization: K. Bailey, Jia Hu
Data curation: K. Bailey, P. Szejner, Brandon Strange, R. K. Monson, Jia Hu

Formal analysis: K. Bailey

Funding acquisition: R. K. Monson, Jia Hu

Writing – original draft: K. Bailey

Writing – review & editing: K. Bailey, P. Szejner, Brandon Strange, R. K. Monson, Jia Hu

The Influence of Winter Snowpack on the Use of Summer Rains in Montane Pine Forests Across the Southwest U.S.

K. Bailey^{1,2} , P. Szejner³ , Brandon Strange^{1,2} , R. K. Monson^{2,4} , and Jia Hu^{1,2}

¹School of Natural Resources and the Environment, University of Arizona, Tucson, AZ, USA, ²Laboratory of Tree Ring Research, University of Arizona, Tucson, AZ, USA, ³Bioeconomy and Environment Unit, Natural Resources Institute Finland, Helsinki, Finland, ⁴Department of Evolutionary Biology, University of Arizona, Tucson, AZ, USA

Abstract A two decade-long megadrought, with likely anthropogenic causes, has impacted forest growth and mortality across the southwestern U.S. Given this event, and the future likelihood of similar climate challenges, it is important to understand how different water resources are used by semi-arid forests in this region. Within the geographic domain of the North American Monsoon climate system, we studied seasonal water-use in eight different *Pinus ponderosa* montane forests distributed across a climate gradient with varying contributions from winter and summer precipitation. We collected oxygen isotopes from precipitation, soil, and xylem water during two contrasting hydrologic years to determine how trees differentially use winter versus summer precipitation sources. Most trees switched from using snowmelt water as the primary source during the early-summer hyper-arid period, to monsoon rainwater during the late-summer. However, during the low snowpack year, which represents the most common climate phenomenon during the megadrought, trees at all sites used less summer rain when compared to the higher snowpack year, demonstrating a drought-induced antecedent influence of winter precipitation on the uptake of summer rain. A possible mechanism to explain the antecedent effect is an earlier snow disappearance during the low snowpack year weakening hydrologic connectivity within the soil profile, decreasing the soil infiltration of summer rains. However, in years with higher snowpack, the snow lasts longer, and this can improve the hydrologic connectivity within the soil profile. As a result, there is more infiltration of summer rains into the soils. This can enhance the maintenance of active shallow fine-root biomass during the period when snowpack disappears, and monsoon rains have yet to arrive. These findings provide insight into how the seasonal interactions between major seasonal climate systems influence forest tree water use in the face of an extreme megadrought.

Plain Language Summary A two decade-long megadrought has impacted forests in the southwestern U.S. The drought has the potential to influence how forests use different proportions of winter and summer precipitation. We examined patterns of tree water use across the North American Monsoon climate region and found that trees generally switched from using snowmelt water during early-summer to monsoon rainwater during late-summer. However, during low snowpack years, trees used less monsoon moisture when compared to higher snowpack years, demonstrating an influence of the previous winter's precipitation on the uptake of current summer rain. Conventional wisdom states that monsoon rains provide relief for drought stressed trees. However, our study shows that decreases in snowpack during the previous winter can impact a trees ability to use summer rain.

1. Introduction

Drought induced forest mortality has increased in the last two decades globally (Allen et al., 2010; Breshears et al., 2005; Hammond et al., 2022; McDowell et al., 2022), and in the southwestern United States, the rapid intensification of a multidecadal megadrought has led to decreases in tree productivity (Williams et al., 2020, 2022). It is likely that climate change will continue to exacerbate the megadrought through increases in winter and summer temperatures, leading to decreases in snowpack and more variable summer precipitation (Hamlet et al., 2005; Knowles et al., 2006; Seager et al., 2007; Seager & Vecchi, 2010). Changes in snowpack extents and duration can influence early spring primary productivity and biogeochemical cycling (Bales et al., 2006; Westerling et al., 2006), which are of great concern for summertime productivity and tree persistence in dryland ecosystems that already exist at the margins of their climate tolerances. In many forests across this region, the arrival of summer rains as a major monsoon climate system contributes to less summertime water stress in forests (Strange et al., 2023), as the rains not only replenish much needed soil moisture during peak summer drought, but the

arrival of the summer moisture also leads to decreases in atmospheric vapor pressure deficit (VPD) (Peltier & Ogle, 2019; Szejner et al., 2016, 2018).

Interannual changes in the relative distributions of winter and summer precipitation across semi-arid landscapes can have significant consequences for plant productivity (Bates et al., 2006; Knapp et al., 2002; Knowles et al., 2020). The timing of soil water recharge and depletion ultimately dictates how precipitation provides plant available water (McNamara et al., 2005; Smith et al., 2011), as plants can both directly use recently fallen precipitation, or use water deeper in the soils that originated from earlier events. In the montane forests of the western U.S., peak soil moisture closely follows the date of snow disappearance (Bales et al., 2011; Harpold et al., 2015), which has been found to be an important source of water for trees in the early spring (Nehemy et al., 2022). Thus, the magnitude and melt timing of snowpack can impact spring and summer available soil moisture (Dwivedi et al., 2023; Hamlet et al., 2007; Tang & Feng, 2001). For example, years with larger snowpack lead to a later melt-out date, culminating in high soil moisture throughout the growing season, while years with smaller snowpack lead to an earlier melt-out date, culminating in low soil moisture throughout the growing season (Kumar et al., 2019; Tang & Feng, 2001). In the southwestern U.S., the impact that summer precipitation has on plant available water depends on antecedent moisture conditions from the previous snowmelt. During large snowpack years when soil moisture remains high through the spring and early summer, summer precipitation can gradually infiltrate into the soil due to high soil hydraulic conductivity; however, during years with low snowpack and drier soil conditions, summer precipitation does not infiltrate as deeply (Kumar et al., 2019; Tang & Feng, 2001). This behavior can be attributed to the non-linear correlation between hydraulic conductivity and soil water content, where a decrease in water content leads to a corresponding reduction in hydraulic conductivity due to a reduction in the interconnectedness of the soil pores (Rossi & Nimmo, 1994). Under low soil water content, water flows via pathways through only thin water films surrounding soil particles, leading to low conductivity. However, under high soil water content, water flows through nearly saturated pore spaces, which greatly increasing hydraulic conductivity. Thus, the interactions between winter and summer precipitation on soil water dynamics, and how that translates to plant-available water complicates our ability to predict how different moisture sources are used by trees across this region.

While the timing and amount of different modes of moisture (e.g., snow and rain) can influence soil moisture throughout the year, a tree's ability to use available soil moisture depends on the depth and distribution of its functional roots, which are physiologically and morphologically responsive to changes in water availability (Ehleringer & Dawson, 1992; Flanagan et al., 1992; Grossiord et al., 2018). Trees with dimorphic root systems, such as the coniferous trees that dominate in montane ecosystems and are the focus of this study, have both shallow (fine) and deep (coarse) roots that allow them to take up soil water at differing depths (Dawson & Pate, 1996; Ehleringer & Dawson, 1992). Past studies have shown that *Pinus ponderosa* trees in the western U.S. can use deep soil water recharged by winter precipitation, as well as shallow soil water recharged by summer precipitation (Eggemeyer et al., 2009; Roden & Ehleringer, 2007; Thomas et al., 2009). In Nebraska, one study found that *P. ponderosa* trees were able to use shallow soil water from spring to mid-summer, which was attributed to the maintenance of fine root production (Eggemeyer et al., 2009). However, in another study in the southwestern U.S., Kerhoulas et al. (2013) found that *P. ponderosa* trees relied less on summer precipitation and mainly used winter precipitation because their functional roots were deployed deeper in the soil. These contrasting studies, all on the same species, but under different precipitation regimes, suggest that montane *P. ponderosa* trees growing in a region with ample snowmelt, but limited summer rain, potentially have different water use strategies than *P. ponderosa* growing in a summer rainfall dominated region. However, these studies, along with others (e.g., Kurpius et al., 2003; Roden & Ehleringer, 2007; Thomas et al., 2009) have examined the water use of *P. ponderosa* within stands isolated to one or two climate types. A comparative study of water-use patterns across multiple sites with contrasting distributions of winter and summer precipitation is missing.

In the southwestern U.S., the North American Monsoon (NAM) climate system delivers ~60% of the annual precipitation during the summer months and the rest is provided as snowmelt in early spring (Figure 1). The bimodal winter and summer precipitation regimes and their respective isotopic signals provide a unique opportunity to examine the reliance of trees on both types of precipitation, an understanding that is lacking in this region. The NAM is most intense in Southern Arizona and New Mexico, with snowpack contributing less to annual precipitation (Adams & Comrie, 1997) (Figure 1). Further north, in Northern Arizona and Southern Utah, the frequency of NAM rains decreases, the depth of snowpack generally increases, and interannual variability in the ratio of winter-to-summer precipitation increases. It is likely that forest stands in the northern periphery

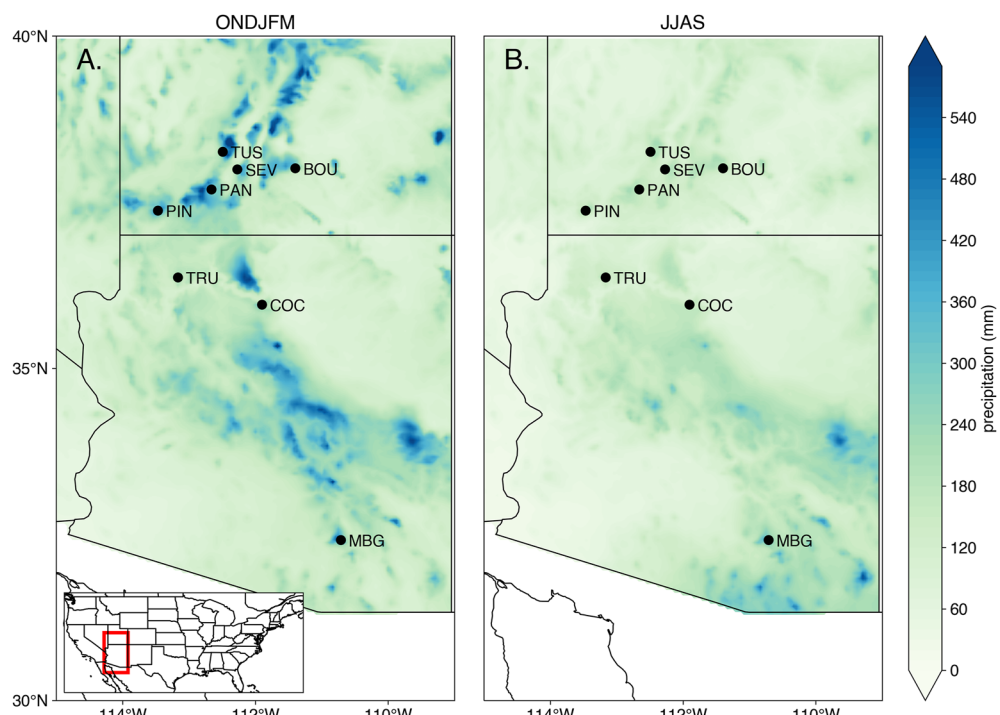


Figure 1. The contribution of winter (a; October–May) and summer (b; June–September) precipitation in the U.S. region of the North American Monsoon domain, where green represents less contribution and blue represents more contribution of winter (a) or monsoon (b) precipitation. Averages for both winter and summer precipitation were calculated from 1960–2018. The black dots represent the locations of tree isotope data collections.

of the NAM domain use both snowmelt and NAM rains for a water source throughout the growing season. Furthermore, with projected increases in aridity in the NAM region (Seager et al., 2007; Seager & Vecchi, 2010), it is likely that these patterns will change in the future. Understanding the relative importance of the timing and amount of winter and summer precipitation in the southwestern U.S. is increasingly important. In this study, we examined tree source water use of eight different *P. ponderosa* forests across a large geographic region to determine how trees use winter and NAM precipitation. We asked: (a) How variable are water use patterns among distinct forests? and (b) Does the amount of winter precipitation in a forest affect its use of summer precipitation?

2. Materials and Methods

2.1. Regional Characteristics

We selected eight montane sites to capture the water use response of different stands of *P. ponderosa* during three seasonal phases, spring (April/May), hyper-arid (June), and summer monsoon (August/September) (Figure 1; Table S1 in Supporting Information S1). The hyper-arid season lies between the spring snowmelt and the late-summer monsoon. It is characterized as an especially hot, dry period with extremely high atmospheric VPD values. Seven sites were selected in the northern periphery of the NAM geographic domain (TUS, SEV, BOU, PAN, PIN, TRU, and COC) (35.96°N , 113.47°W to 38.26°N , 111.40°W), where 20%–40% of annual precipitation occurs during the summer. Hereafter, these are referred to as “the periphery sites.” One reference site (MBG) (32.41°N , 110.71°W) was selected in the core of the U.S. NAM region, where the percentage of summer rains was closer to 50% (Figure 1). Hereafter, this is referred to as ‘the core site’. We obtained daily PRISM estimates of precipitation, temperature, and VPD for the 2017–2018 and 2020–2021 water years (1 October–31 September) for each of the eight sites (PRISM Climate Group, <https://prism.oregonstate.edu>). We used VPD instead of relative humidity because VPD is independent of temperature and better characterizes the driving force of water loss from a plant. To obtain estimates of snow water equivalent (SWE), we used the National Snow and Ice Data Center (NSIDC) 4-km gridded SWE and snow depth data (<https://nsidc.org/data/nsidc-0719/versions/1>; Broxton et al., 2019) and validated it against SNOTEL SWE (Figures S1 and S2 in Supporting Information S1;

USDA Natural Resources Conservation Service, 2022). The NSIDC UA SWE estimates represent interpolated patterns from SNOTEL sites, as well as PRISM and the National Weather Service Cooperative Observer Program (COOP) (Cho et al., 2020). Winter and summer seasonal values were obtained as the sum of the daily PRISM or NSIDC data.

2.2. Tree Sylem, Soil, and Water Isotope Sampling

Tree water use in this region was determined by using the stable isotopes of hydrogen and oxygen ($\delta^2\text{H}$ and $\delta^{18}\text{O}$) (e.g., Brunel et al., 1995; Dawson & Ehleringer, 1991; Eggemeyer et al., 2009; Roden & Ehleringer, 2007; Tang & Feng, 2001). The seasonal water sources are distinguishable in the NAM system because winter precipitation is depleted in the heavier isotopes (^2H and ^{18}O) compared to summer precipitation (Dansgaard, 1964; Flanagan & Ehleringer, 1991; Tulley-Cordova et al., 2021). We note that this differs from other monsoonal climate systems, such as that associated with the Asian monsoon (Hu et al., 2013), in which winter precipitation is isotopically enriched compared to summer precipitation. Using stable hydrogen and oxygen isotope ratios obtained from xylem water, we tracked source water usage of the eight stands of *P. ponderosa* through the three chosen seasonal climate phases. In 2018 and 2021, we sampled the same 110 individual trees (15 at each periphery site, 5 at the core site) during the hyper-arid period (June) and the monsoon period (September). During 2021, we also sampled during spring (April and May) when snowmelt water was dominant in the soils.

During each sampling date, we collected two 5 mm cores from each individual tree at breast height to analyze the stable isotopes of xylem water. Tree cores were placed into glass scintillation vials, sealed with Parafilm to prevent evaporation, and kept cool until samples were brought back to the freezer in the lab. Soil water was also collected at each of the seven periphery sites during the 2021 growing season at the same times during the season that tree xylem samples were collected. A new soil pit was excavated and samples were collected from depths of 5, 25, and 45 cm. All soil samples were also quickly placed in glass scintillation vials, sealed with Parafilm, and were kept cool until they were placed in laboratory freezers. We also collected rainwater in 2021 from May to June (hyper-arid period) and June to August (monsoon period). We placed rain gauges at each of the seven periphery sites, containing a 1 cm layer of mineral oil to prevent evaporation.

We extracted water from the xylem and soil samples using cryogenic water distillation (Ehleringer et al., 2000). Xylem, soil, and precipitation water samples were then analyzed for $^2\text{H}/^1\text{H}$ and $^{18}\text{O}/^{16}\text{O}$ at the University of Utah through the Stable Isotopes Ratio Facility for Environmental Research Lab. The $\delta^2\text{H}$ for xylem water was analyzed by pyrolysis using a high-temperature conversion elemental analyzer (TC/EA) coupled with an isotope ratio mass spectrometer. The $\delta^{18}\text{O}$ for xylem water was analyzed by equilibration with CO_2 and analyzed using a Thermo Finnigan Gas-Bench II connected to a Thermo Finnigan Delta Plus XL. The soil and precipitation samples were analyzed by a Picarro L2130i Analyzer for $\delta^2\text{H}$ and $\delta^{18}\text{O}$. Measured $\delta^2\text{H}$ and $\delta^{18}\text{O}$ values were normalized using the three internal reference materials (DI, EV, and ZE) used during the acquisition and were all calibrated against the international standards of Vienna Standard Mean Ocean Water (V-SMOW) II, GISP, and SLAP. The xylem water samples were analyzed on a Mass Spectrometer to avoid potential organic contaminants, while soil water samples were run using charcoal methods to remove any potential contaminants (Johnson et al., 2017; West et al., 2010). By employing these techniques, we can better control the reliability and accuracy of the measurements.

All ratios were expressed using δ notation ($\delta^2\text{H}$ and $\delta^{18}\text{O}$) with units of parts per thousand (‰) relative to the V-SMOW:

$$\delta^2\text{H} \text{ (or } \delta^{18}\text{O}) = \left(\frac{R_{\text{sample}}}{R_{\text{standard}}} - 1 \right) \times 1,000 \quad (1)$$

where R_{sample} and R_{standard} are the molar ratios of $^2\text{H}/^1\text{H}$ or $^{18}\text{O}/^{16}\text{O}$ of the sample and standard water, respectively. Since it has been found that there can be an offset of up to -10‰ in $\delta^2\text{H}$ between extracted stem water and source water, we opted to focus our analysis mainly on $\delta^{18}\text{O}$, where little to no difference occur between extracted stem water and source water (Chen et al., 2020).

2.3. Statistical Analysis

To test for differences in the $\delta^{18}\text{O}$ of xylem water ($\delta^{18}\text{O}_{\text{xw}}$), we fit a linear mixed-effects ANOVA model using the “ImerTest” package (Kuznetsova et al., 2017) in R (R Core Team, 2022-06-23, R version 4.2.1), with fixed effects

Table 1

The Mean Annual Temperature (°C), Mean Annual VPD_{max} (hPa), Total Monsoon (North American Monsoon (NAM)) Precipitation (mm), Peak Snow Water Equivalent (SWE_{peak}) (mm), and Total Snow Water Equivalent (SWE_{total}) (mm) for Each Site in 2018 and 2021, As Well As the Percent Change From 2018 to 2021 in NAM Precipitation (%), and Total Snow Water Equivalent (%) for Each Site

Site	2018						2021							
	Mean annual temp (°C)	Mean annual max VPD (hPa)	Total NAM precip (mm)	Peak SWE (mm)	Total SWE (mm)	Percent NAM (%)	Mean annual temp (°C)	Mean annual max VPD (hPa)	Total NAM precip (mm)	Peak SWE (mm)	Total SWE (mm)	Percent NAM (%)	Change in NAM (%)	Change in SWE (%)
TUS	7.65	15.08	88.90	29	98	47.57	6.92	15.00	170.69	114	419	28.95	92.00	327.55
SEV	6.02	12.01	137.04	27	94	59.31	5.11	11.43	214.15	79	179	54.89	56.27	87.23
BOU	8.17	14.89	87.00	41	97	47.28	6.99	14.36	211.70	90	208	50.44	143.33	114.43
PAN	7.55	14.23	137.52	31	98	58.39	6.78	13.84	236.56	117	180	56.79	72.02	83.67
PIN	10.05	16.37	168.34	44	120	58.38	9.19	16.59	251.17	99	286	46.76	49.20	138.33
TRU	10.76	19.21	179.03	11	29	86.06	10.05	19.64	157.73	29	73	68.36	-11.90	151.72
COC	10.98	20.63	137.15	16	42	76.56	10.39	20.56	146.84	42	95	60.72	7.07	126.19
MBG	14.13	18.14	290.98	31	64	81.97	12.87	17.04	556.25	20	57	90.71	91.16	-10.94

Note. The sites are listed from most northerly (on top) to most southerly (on bottom).

of site (TUS, SEV, BOU, PAN, PIN, TRU, and COC), period (hyper-arid and monsoon), and year (2018 and 2021). We tested for a three-way interaction between site, period, and year using AIC model selection (Table S2 in Supporting Information S1). Because the samples were collected from the same tree individual every sample period, tree ID was treated as the random effect. We then conducted a post hoc analysis using the “emmeans” package (Lenth, 2022) to obtain estimated marginal means for a pairwise comparison of the three-way interaction. We also used a simple linear regression model to test if the previous year total SWE significantly predicted a switch in source water use from winter to monsoon rains.

3. Results

3.1. Site Climate and Hydrology

During 2018 and 2021, the average annual temperature ranged from 6.02°C to 14.13°C (2018) and 5.11°C–12.87°C (2021), with SEV being the coolest site and MBG being the warmest site (Table 1). The average annual VPD_{max} ranged from 12.01–20.63 hPa (2018) and 11.43–20.56 hPa (2021), with SEV being the wettest and COC being the driest. In 2018, the length of the hyper-arid period was also longer than in 2021, where the number of days between peak SWE (SWE_{peak}) and the on-set of the NAM was two weeks longer during 2018 compared to 2021 (Figure 2).

In general, SWE_{peak} in 2018 was lower than SWE_{peak} in 2021 (Table 1; Figure 2). Across all of the northern sites (TUS, SEV, BOU, PAN, PIN, TRU, COC), SWE_{peak} in 2018 was lower (range of 11.00–44.00 mm) than SWE_{peak} in 2021 (range of 20.00–117.00 mm). However, at the most southern site, MBG, we found the opposite pattern with 2018 SWE_{peak} being 155% higher than 2021 SWE_{peak}.

The timing of snow accumulation and snowmelt were different between the two winter seasons (Figures 2a and 2b). In 2018, snow started to fall in late-December across all sites, while in 2021, snow started to fall during early-November. Snowpack was not consistent for any sites during 2018, but was for TUS, SEV, BOU, PAN, and PIN during 2021. Snowmelt generally started in early to mid-March for both years. However, in 2018 snowmelt had ended before April, while 2021 snowmelt ended the first week in April.

The amount of cumulative NAM precipitation in 2018 was less than the amount of cumulative NAM precipitation in 2021 (Table 1; Figure 2). The total amount of 2018 NAM precipitation ranged from 88.90 to 290.98 mm, with TUS receiving the least amount of precipitation and MBG receiving the most amount of precipitation. The total amount of 2021 NAM precipitation ranged from 146.84 to 556.25 mm, with COC receiving the least amount of precipitation and MBG receiving the most amount of precipitation. For COC, the 2018 total NAM precipitation was slightly lower than the 2021 total (2018 total NAM precipitation was 93% of that for 2021). However, for

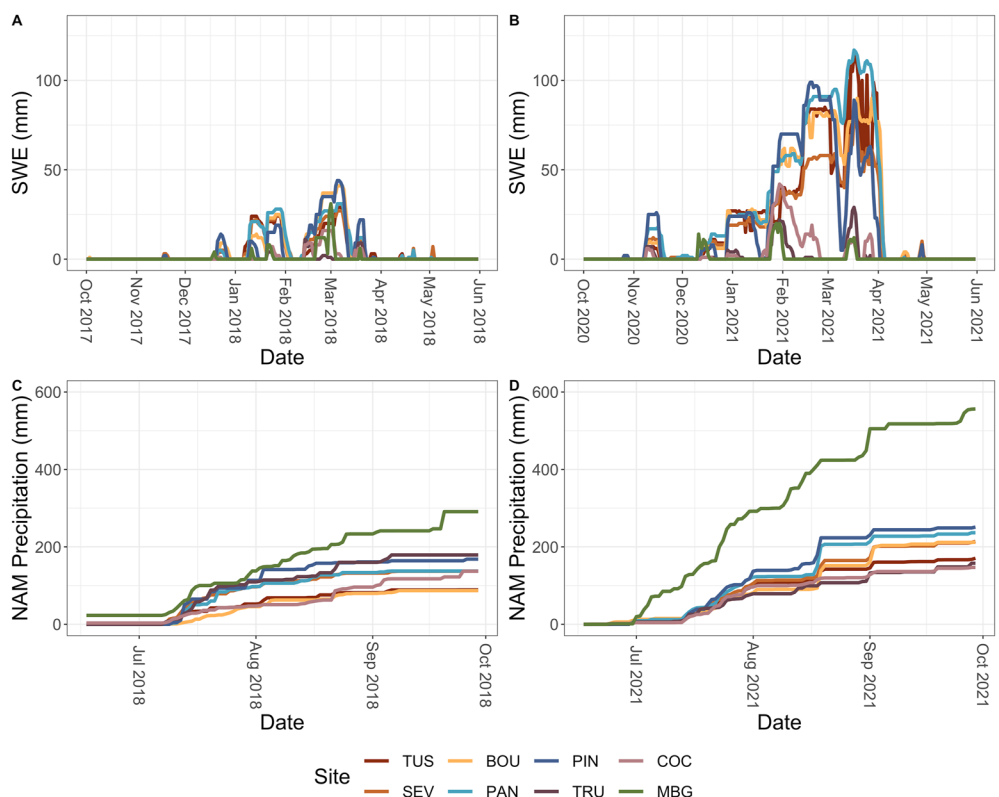


Figure 2. The seasonal water inputs for each of the eight sites, where cumulative snow water equivalent was estimated by National Snow and Ice Data Center data for the year 2018 (a) and 2021 (b). Cumulative precipitation during the North American Monsoon system was estimated using PRISM for 2018 (c) and 2021 (d).

the sites TUS, PAN, SEV, PIN, MBG, and BOU, the 2018 total NAM precipitation was only half of that for 2021 (2018 total monsoon precipitation was 41%–67% of that for 2021). Unlike the other seven sites, TRU experienced greater total monsoon precipitation in 2018 compared to 2021, where total NAM precipitation in 2018 was 113.5% of that for 2021. The onset of the NAM was also different between 2018 and 2021. During 2018, the monsoon season started in mid-July for all the sites except for MBG, where it started in mid-June. In 2021, the monsoon started two weeks earlier in July for all sites.

3.2. Precipitation and Soil Water Isotopes

The $\delta^2\text{H}$ and $\delta^{18}\text{O}$ of precipitation ($\delta^2\text{H}_p$ and $\delta^{18}\text{O}_p$) varied from most depleted early in the growing season to most enriched during the later portions of the growing season (Figures 3 and 4). During the 2021 monsoon season, there was variation in $\delta^{18}\text{O}_p$ across sites where TUS was the least enriched ($-8.16\text{\textperthousand}$), followed by SEV ($-7.60\text{\textperthousand}$), PAN ($-7.30\text{\textperthousand}$), BOU ($-7.12\text{\textperthousand}$), PIN ($-6.55\text{\textperthousand}$), TRU ($-6.05\text{\textperthousand}$), and COC ($-5.60\text{\textperthousand}$) (Figure 4). We used local precipitation oxygen and hydrogen isotopes to establish a local meteoric water line (LMWL) for each of the sites (Figures 4 and 5); however, we were not able to collect $\delta^2\text{H}_p$ and $\delta^{18}\text{O}_p$ isotope from all locations during all periods and we supplemented our data with OIPC 3.0 modeled regional values that were representative for each of the sites (wateriso.utah.edu). However, since the data were limited to a few values, we were unable to address difference in the $\delta^{18}\text{O}$ of precipitation between the two years.

The soil water isotope ($\delta^2\text{H}_s$ and $\delta^{18}\text{O}_s$) profiles with respect to season and soil depth are shown in Figure 4. On average, the spring $\delta^{18}\text{O}_s$ were the most depleted ($-11.62 \pm 2.70\text{\textperthousand}$), while the monsoon $\delta^{18}\text{O}_s$ were most enriched ($-6.40 \pm 4.30\text{\textperthousand}$), with the hyper-arid $\delta^{18}\text{O}_s$ falling between the two ($-8.66 \pm 5.16\text{\textperthousand}$). During the spring, $\delta^{18}\text{O}_s$ for all three soils depths and across all sites were generally more clustered close to the LMWL and did not have a consistent pattern of evaporative enrichment with soil depth (Figure 4; S column). However, during the hyper-arid period, the evaporative enrichment gradient increased in all sites, where the average $\delta^{18}\text{O}_s$ at 5 cm

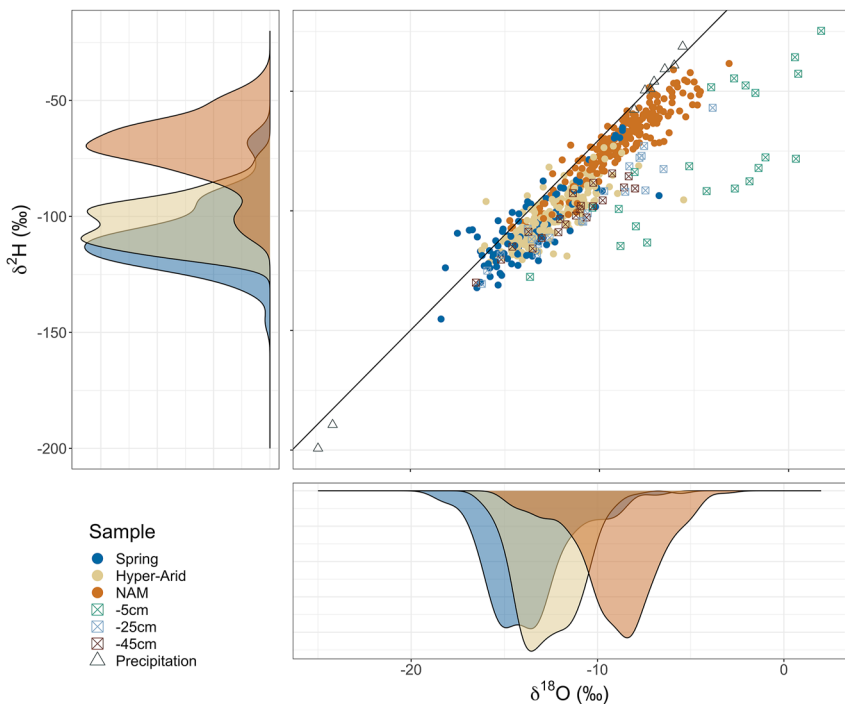


Figure 3. Oxygen ($\delta^{18}\text{O}$) and hydrogen ($\delta^2\text{H}$) isotope data of xylem water during three seasonal periods (spring, hyper-arid, North American Monsoon (NAM)), soil water (5 cm, 25 cm, 45 cm), and precipitation data collected during 2018 and 2021. The black line represents the Global Meteoric Water line. The density plots for the $\delta^2\text{H}$ (left) and $\delta^{18}\text{O}$ (bottom) represent xylem water data for 2018 and 2021 during the spring, hyper-arid, and NAM periods.

was more enriched than $\delta^{18}\text{O}_s$ at 45 cm depth (Figure 4; HA column). During the monsoon period, $\delta^{18}\text{O}_s$ generally shifted to be more isotopically enriched for all soil depths (Figure 4; NAM column), reflecting the infiltration of monsoon precipitation to at least 45 cm in depth (exceptions were BOU, TRU, and COC). Like the spring $\delta^{18}\text{O}_s$ profile, the monsoon soil profile showed a progressive enrichment from the deeper to shallower soil depth, with the upper 5 cm soil value being the most enriched.

3.3. Xylem Water Isotopes

In 2018, the $\delta^{18}\text{O}_{\text{xw}}$ values from BOU, PAN, TRU, COC, and MBG were more isotopically depleted during the hyper-arid period ($-11.49 \pm 1.13\text{\textperthousand}$) compared to the NAM period ($-7.96 \pm 1.69\text{\textperthousand}$) (signifying switch from winter snowmelt water use to NAM precipitation), while TUS, SEV, and PIN did not differ in $\delta^{18}\text{O}_{\text{xw}}$ from the hyper-arid to monsoon period (signifying no switch in water use) (Tables S3 and S4 in Supporting Information S1) (Figures 3 and 5). To better visualize the switch in source water use from winter to summer precipitation, we also subtracted the hyper-arid $\delta^{18}\text{O}_{\text{xw}}$ from the monsoon $\delta^{18}\text{O}_{\text{xw}}$ ($\delta^{18}\text{O}_{\text{diff}} = \text{monsoon } \delta^{18}\text{O}_{\text{xw}} - \text{hyper-arid } \delta^{18}\text{O}_{\text{xw}}$). Positive $\delta^{18}\text{O}_{\text{diff}}$ values represent shifts in source water use. Among all the sites, MBG had the greatest $\delta^{18}\text{O}_{\text{diff}}$ ($4.36 \pm 0.84\text{\textperthousand}$), followed by COC ($4.10 \pm 1.80\text{\textperthousand}$), PAN ($3.70 \pm 1.00\text{\textperthousand}$), BOU ($3.17 \pm 1.19\text{\textperthousand}$), TRU ($2.93 \pm 2.21\text{\textperthousand}$), PIN ($1.50 \pm 0.78\text{\textperthousand}$), SEV ($1.29 \pm 2.38\text{\textperthousand}$), and TUS ($0.41 \pm 2.05\text{\textperthousand}$) (Figure 6).

In 2021, the $\delta^{18}\text{O}_{\text{xw}}$ values from all the sites were more isotopically depleted during the hyper-arid period ($-13.45 \pm 1.48\text{\textperthousand}$) compared to the monsoon period ($-8.64 \pm 1.82\text{\textperthousand}$) (Figure 5), even at the sites TUS, SEV, and PIN, which did not demonstrate a consistent switch in $\delta^{18}\text{O}_{\text{xw}}$ during 2018 (indicating trees in all sites switched water use from snowmelt to NAM precipitation) (Tables S3 and S4 in Supporting Information S1). When assessing the switch in water source use from winter to summer precipitation, $\delta^{18}\text{O}_{\text{diff}}$, COC had the greatest $\delta^{18}\text{O}_{\text{diff}}$ ($7.07 \pm 1.42\text{\textperthousand}$), followed by PAN ($6.07 \pm 1.30\text{\textperthousand}$), TUS ($5.07 \pm 1.82\text{\textperthousand}$), BOU ($4.87 \pm 0.78\text{\textperthousand}$), PIN ($4.54 \pm 1.23\text{\textperthousand}$), TRU ($3.84 \pm 1.20\text{\textperthousand}$), SEV ($3.04 \pm 1.03\text{\textperthousand}$), and MBG ($1.63 \pm 0.81\text{\textperthousand}$) (Figure 6).

We found a significant difference in the seasonal differences in $\delta^{18}\text{O}_{\text{xw}}$ between the monsoon versus hyper-arid periods, ($F_{1,284.18} = 1,080.73, p < 0.0001$), suggesting a switch in water source use from winter precipitation (from the $\delta^{18}\text{O}_{\text{xw}}$ collected during the hyper-arid period) to monsoon precipitation (from $\delta^{18}\text{O}_{\text{xw}}$ collected during the

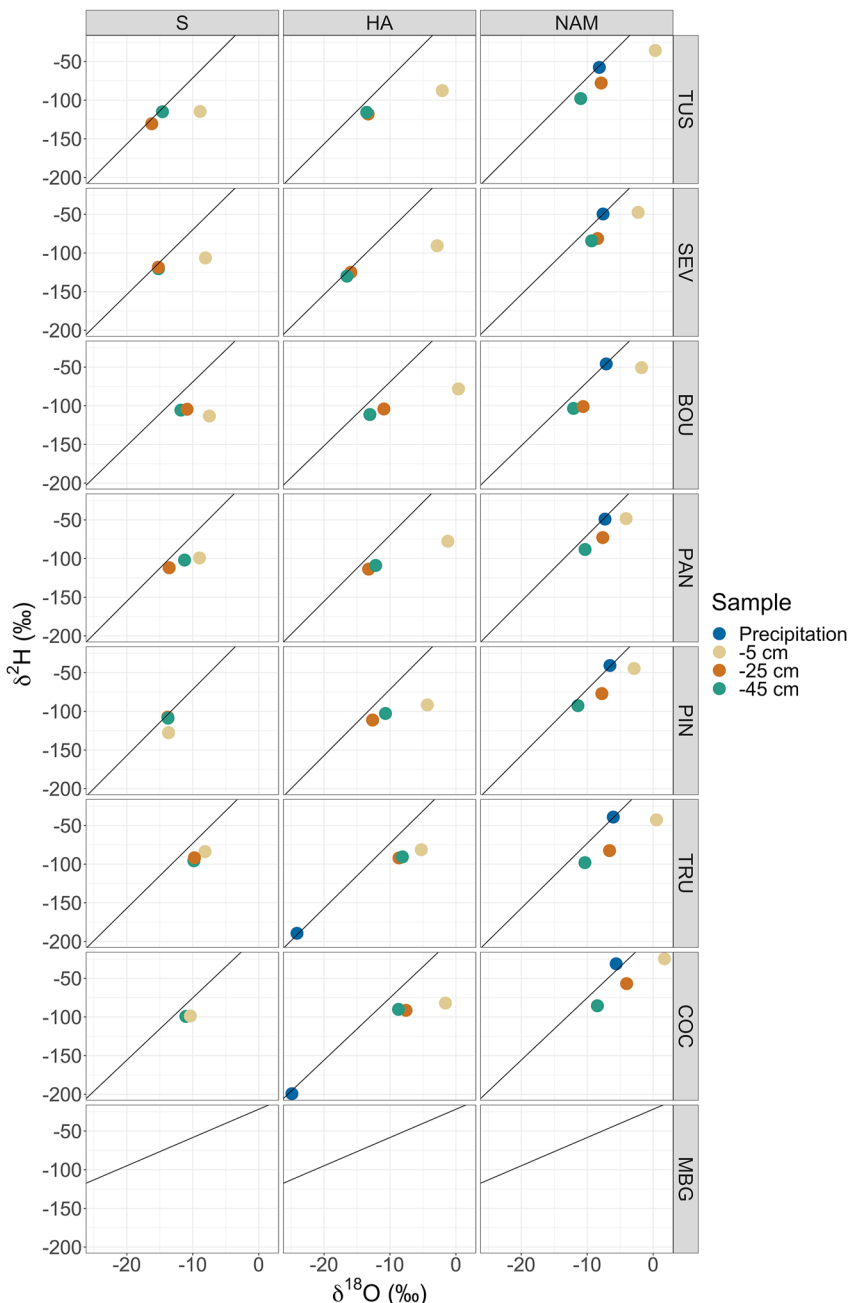


Figure 4. Soil water and precipitation isotopes from the 2021 growing season. For each site, there were three hydroclimate periods: spring (S), hyper-arid (HA), and monsoon (North American Monsoon). The black line represents the local meteoric water line estimated from the modeled OIPC 3.0 monthly average $\delta^{18}\text{O}$ and $\delta^2\text{H}$ precipitation data. We were unable to collect soil water or precipitation data for MBG for 2021.

monsoon period). The change in $\delta^{18}\text{O}_{\text{sw}}$ from winter precipitation to monsoon precipitation was different for each of the sites (period \times site interaction; $F_{6,284.17} = 17.54, p < 0.001$), suggesting some sites had a stronger switch from winter precipitation water use to monsoon precipitation water use compared to other sites. We also found a site \times year interaction ($F_{6,284.09} = 3.20, p = 0.004$), suggesting the trees at each site were using water differently between the 2 years. Additionally, we found a period \times year interaction ($F_{1,285.37} = 130.14, p < 0.0001$), suggesting that the change in $\delta^{18}\text{O}_{\text{sw}}$ from winter precipitation to monsoon precipitation was different for each year. We also found a three-way interaction among year \times site \times period ($F_{6,285.32} = 3.51, p = 0.0023$) (Table S2 in Supporting Information S1).

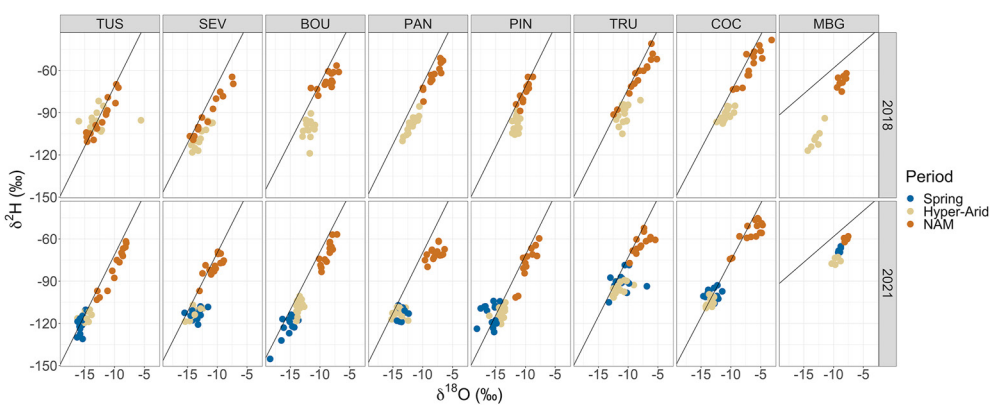


Figure 5. Oxygen ($\delta^{18}\text{O}$) and hydrogen ($\delta^2\text{H}$) isotope data of xylem water for each tree during the spring, hyper-arid, and monsoon (North American Monsoon) periods for 2018 (top) and 2021 (bottom) season at each of the eight sites. The black line is the local meteoric line calculated for each site estimated from the modeled OIPC 3.0 monthly average $\delta^{18}\text{O}$ and $\delta^2\text{H}$ precipitation data.

There was a significant relationship between SWE_{peak} (and $\text{SWE}_{\text{total}}$) during the previous winter/current year spring and the NAM use (as indicated by $\delta^{18}\text{O}_{\text{diff}}$) in the subsequent summer (Figure 7). Across all sites, greater SWE (both in peak and total) led to a greater tendency to switch from winter to summer precipitation use ($F_{1,211} = 41.37$, $p < 0.0001$ for SWE_{peak} ; $F_{1,211} = 18.06$, $p < 0.0001$ for $\text{SWE}_{\text{total}}$).

4. Discussion

In this study, we examined the water sources used by *P. ponderosa* forest stands near the northern boundary of the NAM climate system domain to better understand how these forests use winter versus summer precipitation and how that usage might respond to an intensification of the southwestern U.S. megadrought. We chose seven of the sites to be within a narrow latitudinal band (within 2° latitude; Figure 1) of each other to examine the degree of site variance that exists in winter versus summer precipitation use that is not influenced by significant latitudinal effects. A reference site was chosen closer to the core of the NAM climate system and near the arid southernmost boundary of *P. ponderosa* ecosystems. The NAM climate system develops across a clear latitudinal span each year, progressing northward from its incipient formation in the Sierra Madre Occidental mountains of northwestern Mexico, typically in late-May, to its ultimate destination in northern Arizona and southern Utah, where it dissipates by mid-September (Barlow et al., 1998). In northern Arizona, near the northern boundary of the

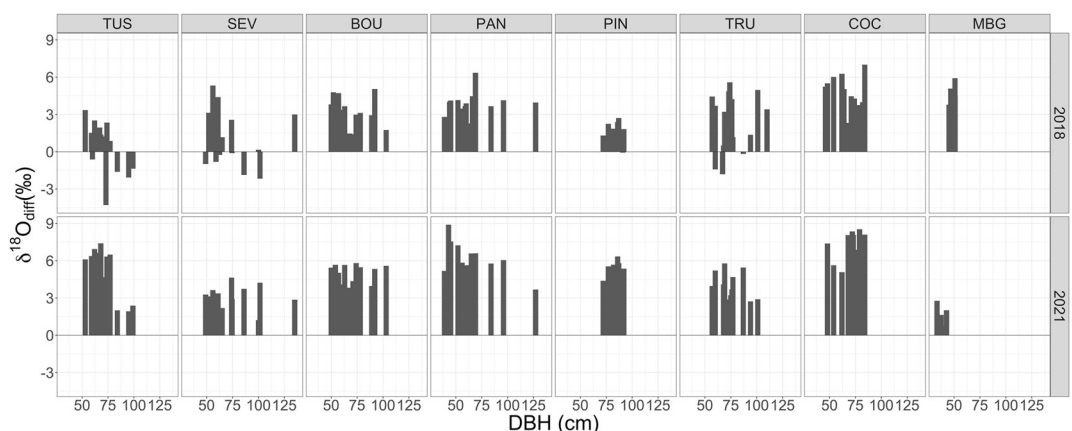


Figure 6. The difference in the xylem water oxygen isotope ($\delta^{18}\text{O}_{\text{wx}}$) for each tree during the hyper-arid period ($\delta^{18}\text{O}_{\text{HA}}$) and after the start of the monsoon ($\delta^{18}\text{O}_{\text{NAM}}$) for the 2018 and 2021 ($\delta^{18}\text{O}_{\text{diff}} = \delta^{18}\text{O}_{\text{NAM}} - \delta^{18}\text{O}_{\text{HA}}$). Positive values indicated a change from snowmelt dominated source water signal to a monsoon dominated source water signal. Zero or negative values indicate a continued use of snowmelt dominated source water signal from the hyper-arid period through the start of the monsoon.

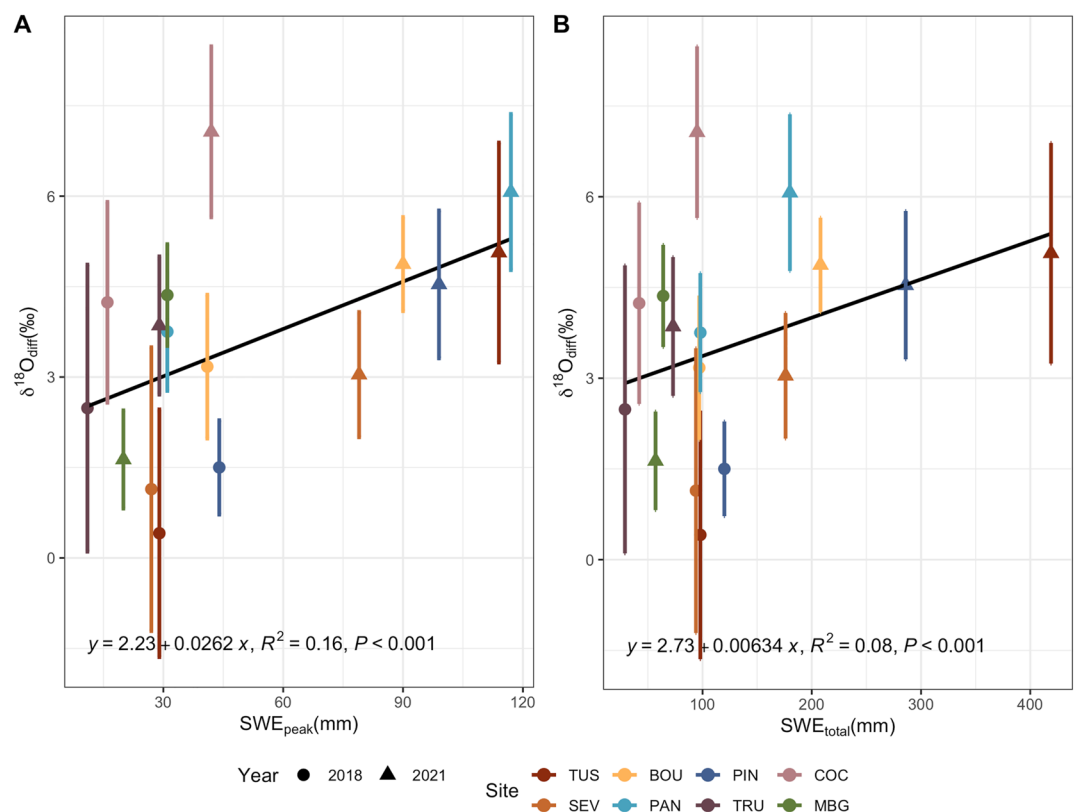


Figure 7. The relationship between the relative difference in xylem water oxygen isotope from summer North American Monsoon and hyper-arid periods ($\delta^{18}\text{O}_{\text{diff}} = \delta^{18}\text{O}_{\text{NAM}} - \delta^{18}\text{O}_{\text{HA}}$) and SWE_{peak} (a) or SWE_{total} (b; October–April). Each dot (2018)/triangle (2021) represents the mean $\delta^{18}\text{O}_{\text{diff}}$ at each site with the standard deviation. The black line represents the linear relationship between SWE_{peak} (or SWE_{total}) and $\delta^{18}\text{O}_{\text{diff}}$ for all the trees in each site.

system, the convective nature of NAM rains interacts with a sharp change in topography, from the low-elevation plains of the southern deserts to the high relief of the Mogollon Rim and Colorado Plateau (Higgins et al., 1997). Two of our sites (COC and TRU) lie at the southern edge of this sharp change in topography, and are characterized by lesser amounts of winter snow, compared to the other five sites. The core site (MBG) served as a southern anchor for the gradient and lies $\sim 5^{\circ}$ – 6° of latitude south of the other seven sites. It is in the Santa Catalina Mountains north of Tucson, Arizona, which are part of the forested “island” mountains, often called Sky Islands, that emerge from arid lowland landscapes of the Sonoran Desert. When taken together, the group of sites that we assembled provides an unprecedented opportunity to examine precipitation variation and its use by trees in semi-arid montane forests.

With these site-specific and seasonal differences in mind, we found that trees in all but three of the most northern sites switched from using snowmelt water during the early-summer to monsoon rainwater during the late-summer during the drier year, and trees at all sites switched during the wetter year. While there is reason for intuitive acceptance of this observation, given the large geographic expanse of *P. ponderosa* and the variable findings from past studies, we did not assume this to be the case at the start of the study. Our results were consistent with some studies in which *P. ponderosa* did switch water source use between spring and summer. Eggemeyer et al. (2009) observed a switch from deeper to shallower soil water in a 65-year-old *P. ponderosa* plantation from a single site in the Sandhills of Nebraska. Roden and Ehleringer (2007) compared the $\delta^{18}\text{O}$ of latewood cellulose in *P. ponderosa* growing in three different stands, in Arizona, California, and Oregon. They found an increase in the $\delta^{18}\text{O}$ of latewood in the Arizona forest, compared to the others which received less NAM rain, also suggesting the switch to the use of summer monsoon rain. However, given the limitations of the study’s experimental design, Roden and Ehleringer (2007) found no observed trends in latewood $\delta^{18}\text{O}$ with interannual differences in summer rain. Thomas et al. (2009) studied *P. ponderosa* in central Oregon, where summer monsoon rain is absent, and found evidence of a seasonal switch between deeper and shallower water sources, though the direction of the switch was

opposite to the pattern we observed. In the Oregon forest, trees used shallower water early in the season, presumably from snowmelt, and switched to deeper sources later in the summer, as the soil profile dried downward. However, the findings from our study were opposite to a previous study that was conducted closer to our sites in Northern Arizona. Using similar isotopic approaches, Kerhoulas et al. (2013) observed no evidence of significant use of summer monsoon precipitation. Both older (>100 years) and younger (50–60 years) trees relied almost exclusively on deeper water sources with isotopic composition reflecting winter snow. Given the disparate, and in some cases, conflicting, results of these past studies, and their restriction to a few widely separated sites, there simply was not a basis on which to generalize about forest water use in montane ecosystems of the western U.S. Thus, our study has significance in providing deeper insight into the patterns of water use across a broader set of sites with greater variance among sites in the amounts of winter and summer precipitation.

The differences in the degree of source-water adjustment between 2018 and 2021 in some of the stands suggest an extrinsic interaction between the relative distributions of winter and summer precipitation conditions. We posit that this interaction is due to wetter winters facilitating a tree's ability to use summer precipitation (Figure 7). We expand upon this hypothesis in the following section.

4.1. Seasonal Precipitation Inputs and Tree Water Use

In general, 2021 was a wetter year than 2018, both in winter and summer monsoon precipitation. However, we would like to point out that 2021 was still considered a drought year, and part of the ongoing southwestern U.S. megadrought (Williams et al., 2022). At all seven of the sites at the northern edge of the NAM domain, SWE_{peak} was considerably greater in 2021, compared to 2018, resulting in a later snowmelt (snow disappearance was later in 2021 than in 2018) (Table 1; Figures 2a and 2b). The larger snowpack in 2021, combined with a longer melt-out period led to soils remaining wet for a longer period of time (Figure S3 in Supporting Information S1; Harpold et al., 2015; McNamara et al., 2005). Additionally, at all sites in 2021, the monsoon rains started two weeks earlier than in 2018 (Figures 2c and 2d), which would have further contributed to more mesic conditions compared to 2018 and led to wetter soils and lower VPD throughout the entire summer. These conditions also likely enhanced plant available water (McNamara et al., 2005). These two contrasting hydrologic years have provided a unique natural experiment within which to examine plant water use, as it allowed us to assess the complex interactions between winter and summer precipitation on plant available water.

Fine roots play an essential role in a tree's water uptake and transport because they can be physiologically and morphologically responsive to changes in water availability (Flanagan et al., 1992; Grossiord et al., 2017). If trees experience prolonged dry periods where the soil water potential drops below the permanent wilting point, roots can become dehydrated and may even be shed (McCormack & Guo, 2014). Root shedding reduces the effective surface area of the root system, which can limit the tree's ability to absorb water when the soil becomes wet again. Even when soil moisture content returns to a sufficient level, there can be a delay in the growth of fine roots, once again, reducing a tree's ability to respond quickly to increases in water availability (McCormack & Guo, 2014). We hypothesize that during the drier year of 2018, low snowpack and early melt caused dry soils during the early summer and reduced the ability of trees to quickly respond to the summer water source (Figure 6). During the wetter year of 2021, in contrast, the effect of moist spring soils likely extended the period of water availability later into the hyper-arid period, allowing the trees to respond more quickly to the eventual onset of the NAM. If this hypothesis is correct, the state of the fine root surface area of trees at the onset of the NAM has an important impact on seasonal linkages between the use of winter and summer precipitation sources. The extent to which extended droughts, much like the current megadrought, influence fine root maintenance during the hyper-arid period could represent a significant vulnerability in semi-arid forests of western North America and is worth investigation in future studies. For example, Urrutia-Jalabert et al. (2023) have observed that forests in Central Chile are maintaining their growth rates, despite an ongoing megadrought, by shifting their source water use to deeper pools of water. However, the role of forest cover characteristics and soil properties in mediating the effects of prolonged droughts should not be overlooked. As Dwivedi et al. (2023) illustrates, factors such as tree density and snow accumulation patterns can significantly influence root stress and the infiltration capacity of soils. It is vital to incorporate these variables in future studies to develop a comprehensive understanding of forest response to extreme and prolonged drought conditions.

4.2. Antecedent Effects Involving Winter and Summer Precipitation

Previous studies have shown that *P. ponderosa* have a high degree of water use plasticity (Bowling et al., 2003; Kerhoulas et al., 2013; Marshall & Monserud, 2006; Roden & Ehleringer, 2007), and the explanations were based

on precipitation inputs; in years with a large snowpack and/or late snowmelt, trees used more winter precipitation, while years with large summer rainfall, trees used more summer rains. Our results show that this perspective is too simplistic because summer soil moisture is dependent not only on summer precipitation inputs, but also antecedent soil moisture conditions from the winter and spring. The antecedent moisture conditions that are established in the soils due to winter precipitation can influence the trees' ability to use summer rains. In a recent study, Martin et al. (2018) found that within a watershed in western Montana, Douglas fir trees growing in lower elevations (that received less winter snowpack) used snowmelt water at a greater fraction of total growing-season water use, than trees growing in higher elevations (that received more winter snowpack). That is, even though higher elevation trees received more than 50% more snowfall, trees growing at the higher elevations had more of a summer rainfall isotopic signal and less of a winter snowpack signal. In another study in a high elevation conifer forest in SW Colorado that receives high snowfall, Berkelhammer et al. (2020) observed all conifers to quickly switch to summer rain use. However, it is important to note that Berkelhammer et al. (2020) used cellulose $\delta^{18}\text{O}$ and was conducted in a snow-dominated region, which differs from our study. Nevertheless, in both Martin et al. (2018) and Berkelhammer et al. (2020), the large snowpack appears to keep soils wet for longer during the spring and into the summer, thereby facilitating summer precipitation water use.

Although we observed most of the trees from our study switched from winter to summer precipitation water use, there were some trees in three sites, TUS, SEV, and PIN, that did not show a change in $\delta^{18}\text{O}_{\text{sw}}$ during 2018 but did during 2021. These results are consistent with a failure to use monsoon precipitation during the dry-winter year (2018), but a success during the wet-winter year (2021) (Figures 5 and 6). The results cannot be explained by differences in summer precipitation alone, but can be explained by interactions between winter precipitation (i.e., SWE_{peak}) and summer precipitation (i.e., monsoon rain). For example, in 2018, some trees at TUS did not switch water source use, but they did in 2021, even though the summer monsoon rains were only slightly more compared to 2018 (Table 1). The greater difference was that SWE_{peak} in 2018 was 75% lower than that of 2021. In contrast, some sites switched source water use during both years, even with less summer monsoon input. For example, TRU received twice the SWE_{peak} in 2021 compared to 2018, but received less monsoon precipitation during 2021; nevertheless, trees from TRU in 2021 still switched from a snowmelt water source to a monsoon water source during the summer monsoon period. The water use responses in these forests support our reasoning that wet winters can help facilitate the use of summer rains in ponderosa pines. While we used a simplistic view on a switch in source water that did not account for potential errors that could affect the isotopic composition of source water use, for example, winter snowpack sublimation, lack of higher temporal resolution in precipitation isotopes, variation in rooting depth and depth in which trees access water, we still found a statistically significant relationship between snowpack and a switch from winter to summer precipitation water use in these forests. Thus, with expected decreases in snowpack and more variable summer precipitation (Hamlet et al., 2005; Knowles et al., 2006; Seager et al., 2007; Seager & Vecchi, 2010), this can greatly impact if and how these trees use summer monsoon rains.

We believe that wet winters increase a trees ability to take advantage of summer rains through summer water infiltration patterns and hydrologic connectivity within the soil profile, which led to the maintenance of fine root activity during the hyper-arid period. During years with low snowpack, the shallow soil layers become dry earlier, leading low soil water potential and low soil hydraulic conductivity. As a result, fine roots may become inactive and even senesce. In contrast, during years with a higher snowpack the shallow soil layers remain wet for longer, leading to higher soil water potential and higher hydraulic conductivity, which can maintain fine root activity. When the NAM rains do arrive, the higher hydraulic conductivity can transmit the precipitation deeper into the soil layers (Bowyer-Bower, 1993) and the fine roots will be able to take up more summer precipitation. During the wet year (2021), we found this to be the case (Figure 4). In all of our sites, soils 25 cm and below showed a NAM isotope signal during the late summer, suggesting that larger snowpack led to higher hydraulic conductivity in the soils, which likely kept the shallow fine roots active, allowing these trees to take up monsoon precipitation (Figure 4) (Berkelhammer et al., 2020; Kumar et al., 2019).

As climate change continues to impact the hydroclimate in the western U.S. (Seager et al., 2007) and likely extend the megadrought, understanding the interactions between winter and summer precipitation on plant available water is important. While summer rains can provide relief for water stressed trees, our study indicates that decreases in snowpack can impact a trees ability to use that summer rain. In a region such as the North American monsoon region where plants rely on both winter and summer precipitation, changes to one or both of these

different moisture supplies can have large impacts on a plants ability to use different pools of soil moisture and ultimately alter a plants ability to cope with water stress.

5. Conclusions

Our study suggests that potentially complex interactions between winter and summer climate systems have important influences on how trees in semi-arid montane forests use water. These findings demonstrated that during a low snowpack year, trees found in the northern periphery of the monsoon region used less monsoon precipitation than during a high snowpack year. This result was consistent across multiple distinct forest sites. We believe this is because a shallow snowpack does not provide sufficient snowmelt to keep soil moisture elevated and the fine roots active until the arrival of the monsoon rains. However, during a higher snowpack year, higher soil hydraulic conductivity allowed summer precipitation to infiltrate into the soils and be utilized by the trees. Our results provide important new insights on how the interaction between winter and summer precipitation can help us assess the impact that a continuing megadrought will have on plant water uptake.

Conflict of Interest

The authors declare no conflicts of interest relevant to this study.

Data Availability Statement

Data for this manuscript is published in the EDI Data Repository and are publicly accessible through the EDI Data Portal (Hu, 2023).

Acknowledgments

This work was supported by the Macrosystems program in the Emerging Frontiers section of the U.S. National Science Foundation (NSF award 1065790) and the Ecosystems Program in the Division of Environmental Biology (NSF Award 1754430). KB and JH conceived the research idea. KB, PS, BS, and JH collected the data. KB performed the data analyses and wrote the initial draft. KB, PS, BS, RKM, and JH edited subsequent drafts of the manuscript.

References

Adams, D. K., & Comrie, A. C. (1997). The North American monsoon. *Bulletin of the American Meteorological Society*, 78(10), 2197–2213. [https://doi.org/10.1175/1520-0477\(1997\)078<2197:TNAM>2.0.CO;2](https://doi.org/10.1175/1520-0477(1997)078<2197:TNAM>2.0.CO;2)

Allen, C. D., Macalady, A. K., Chenchouni, H., Bachelet, D., McDowell, N., Vennetier, M., et al. (2010). A global overview of drought and heat-induced tree mortality reveals emerging climate change risks for forests. *Forest Ecology and Management*, 259(4), 660–684. <https://doi.org/10.1016/j.foreco.2009.09.001>

Bales, R. C., Hopmans, J. W., O'Geen, A. T., Meadows, M., Hartsough, P. C., Kirchner, P., et al. (2011). Soil moisture response to snowmelt and rainfall in a Sierra Nevada mixed-conifer forest. *Vadose Zone Journal*, 10(3), 786–799. <https://doi.org/10.2136/vzj2011.10001>

Bales, R. C., Molotch, N. P., Painter, T. H., Dettinger, M. D., Rice, R., & Dozier, J. (2006). Mountain hydrology of the western United States. *Water Resources Research*, 42(8), 1–13. <https://doi.org/10.1029/2005WR004387>

Barlow, M., Nigam, S., & Berbery, E. H. (1998). Evolution of the North American monsoon system. *Journal of Climate*, 11(9), 2238–2257. [https://doi.org/10.1175/1520-0442\(1998\)011<2238:EOTNAM>2.0.CO;2](https://doi.org/10.1175/1520-0442(1998)011<2238:EOTNAM>2.0.CO;2)

Bates, J. D., Svejcar, T., Miller, R. F., & Angell, R. A. (2006). The effects of precipitation timing on sagebrush steppe vegetation. *Journal of Arid Environments*, 64(4), 670–697. <https://doi.org/10.1016/j.jaridenv.2005.06.026>

Berkelhammer, M., Still, C. J., Ritter, F., Winnick, M., Anderson, L., Carroll, R., et al. (2020). Persistence and plasticity in conifer water-use strategies. *Journal of Geophysical Research: Biogeosciences*, 125(2), 1–20. <https://doi.org/10.1029/2018JG004845>

Bowling, D. R., McDowell, N. G., Welker, J. M., Bond, B. J., Law, B. E., & Ehleringer, J. R. (2003). Oxygen isotope content of CO₂ in nocturnal ecosystem respiration: 2. Short-Term dynamics of foliar and soil component fluxes in an old-growth ponderosa pine forest. *Global Biogeochemical Cycles*, 17(4), 1–12. <https://doi.org/10.1029/2003gb002082>

Bowyer-Bower, T. A. S. (1993). Effects of rainfall intensity and antecedent moisture on the steady-state infiltration rate in a semi-arid region. *Soil Use & Management*, 9(2), 69–75. <https://doi.org/10.1111/j.1475-2743.1993.tb00932.x>

Breshears, D. D., Cobb, N. S., Rich, P. M., Price, K. P., Allen, C. D., Balice, R. G., et al. (2005). Regional vegetation die-off in response to global-change-type drought. *Proceedings of the National Academy of Sciences of the United States of America*, 102(42), 15144–15148. <https://doi.org/10.1073/pnas.0505734102>

Broxton, P., Zeng, X., & Dawson, N. (2019). Daily 4 km gridded SWE and snow depth from assimilated in-situ and modeled data over the conterminous US, version 1 [Dataset]. NASA National Snow and Ice Data Center Distributed Active Archive Center. <https://doi.org/10.5067/0GGPB220EX6A>

Brunel, J.-P., Walker, G. R., & Kennett-Smith, A. K. (1995). Field validation of isotopic procedures for determining sources of water used by plants in a semi-arid environment. *Journal of Hydrology*, 167(1–4), 352–368. <https://doi.org/10.1093/eurheartj/ehu219>

Chen, Y., Helliker, B. R., Tang, X., Li, F., Zhou, Y., & Song, X. (2020). Stem water cryogenic extraction biases estimation in deuterium isotope composition of plant source water. *Proceedings of the National Academy of Sciences of the United States of America*, 117(52), 33345–33350. <https://doi.org/10.1073/PNAS.2014422117>

Cho, E., Jacobs, J. M., & Vuyovich, C. M. (2020). The value of long-term (40 years) airborne gamma radiation SWE record for evaluating three observation-based gridded SWE data sets by seasonal snow and land cover classifications. *Water Resources Research*, 56(1), 1–23. <https://doi.org/10.1029/2019WR025813>

Dansgaard, W. (1964). Stable isotopes in precipitation. *Tellus*, 16(4), 436–468. <https://doi.org/10.3402/tellusa.v16i4.8993>

Dawson, T. E., & Ehleringer, J. R. (1991). Streamside trees that do not use stream water. *Nature*, 350(6316), 335–337. <https://doi.org/10.1038/350335a0>

Dawson, T. E., & Pate, J. S. (1996). Seasonal water uptake and movement in root systems of Australian phreatophytic plants of dimorphic root morphology: A stable isotope investigation. *Oecologia*, 107(1), 13–20. <https://doi.org/10.1007/bf00582230>

Dwivedi, R., Biederman, J. A., Broxton, P. D., Lee, K., Leeuwen, W. J. D. V., & Pearl, J. K. (2023). Forest density and snowpack stability regulate root zone water stress and percolation differently at two sites with contrasting ephemeral vs. stable seasonal snowpacks. *Journal of Hydrology*, 624(June), 129915. <https://doi.org/10.1016/j.jhydrol.2023.129915>

Eggemeyer, K. D., Awada, T., Harvey, F. E., Wedin, D. A., Zhou, X., & Zanner, C. W. (2009). Seasonal changes in depth of water uptake for encroaching trees *Juniperus virginiana* and *Pinus ponderosa* and two dominant C₄ grasses in a semiarid grassland. *Tree Physiology*, 29(2), 157–169. <https://doi.org/10.1093/treephys/tpn019>

Ehleringer, J. R., & Dawson, T. E. (1992). Water uptake by plants: Perspectives from stable isotope composition. *Plant, Cell and Environment*, 15(9), 1073–1082. <https://doi.org/10.1111/j.1365-3040.1992.tb01657.x>

Ehleringer, J. R., Roden, J., & Dawson, T. E. (2000). Assessing ecosystem-level water relations through stable isotope ratio analyses. In O. E. Sala, R. B. Jackson, H. A. Mooney, & R. W. Howarth (Eds.), *Methods in ecosystem science* (pp. 181–198). Springer New York. https://doi.org/10.1007/978-1-4612-1224-9_13

Flanagan, L. B., & Ehleringer, J. R. (1991). Stable isotope composition of stem and leaf water: Applications to the study of plant water use. *Functional Ecology*, 5(2), 270. <https://doi.org/10.2307/2389264>

Flanagan, L. B., Ehleringer, J. R., & Marshall, J. D. (1992). Differential uptake of summer precipitation among co-occurring trees and shrubs in a pinyon-juniper woodland. *Plant, Cell and Environment*, 15(7), 831–836. <https://doi.org/10.1111/j.1365-3040.1992.tb02150.x>

Grossiord, C., Sevanto, S., Bonal, D., Borrego, I., Dawson, T. E., Ryan, M., et al. (2018). Prolonged warming and drought modify belowground interactions for water among coexisting plants. *Tree Physiology*, 39(1), 55–63. <https://doi.org/10.1093/treephys/tpy080>

Grossiord, C., Sevanto, S., Dawson, T. E., Adams, H. D., Collins, A. D., Dickman, L. T., et al. (2017). Warming combined with more extreme precipitation regimes modifies the water sources used by trees. *New Phytologist*, 213(2), 584–596. <https://doi.org/10.1111/nph.14192>

Hamlet, A. F., Mote, P. W., Clark, M. P., & Lettenmaier, D. P. (2005). Effects of temperature and precipitation variability on snowpack trends in the Western United States. *Journal of Climate*, 18(21), 4545–4561. <https://doi.org/10.1175/JCLI3538.1>

Hamlet, A. F., Mote, P. W., Clark, M. P., & Lettenmaier, D. P. (2007). Twentieth-century trends in runoff, evapotranspiration, and soil moisture in the western United States. *Journal of Climate*, 20(8), 1468–1486. <https://doi.org/10.1175/JCLI4051.1>

Hammond, W. M., Williams, A. P., Abatzoglou, J. T., Adams, H. D., Klein, T., López, R., et al. (2022). Global field observations of tree die-off reveal hotter-drought fingerprint for Earth's forests. *Nature Communications*, 13(1), 1761. <https://doi.org/10.1038/s41467-022-29289-2>

Harpold, A. A., Molotch, N. P., Musselman, K. N., Bales, R. C., Kirchner, P. B., Litvak, M., & Brooks, P. D. (2015). Soil moisture response to snowmelt timing in mixed-conifer subalpine forests. *Hydrological Processes*, 29(12), 2782–2798. <https://doi.org/10.1002/hyp.10400>

Higgins, W., Yao, Y., & Wang, X. L. (1997). Influence of the North American Monsoon System on the U. S. summer precipitation regime. *American Meteorological Society*, 10(10), 2600–2622. [https://doi.org/10.1175/1520-0442\(1997\)010<2600:iotnam>2.0.co;2](https://doi.org/10.1175/1520-0442(1997)010<2600:iotnam>2.0.co;2)

Hu, J. (2023). *Xylem water oxygen and hydrogen isotopes of Ponderosa Pine trees and soil samples in the southwestern U.S. 2018 and 2021 version 1*. Environmental Data Initiative. <https://doi.org/10.6073/pasta/228e95361360f107c572781250ca028e>

Hu, J., Hopping, K. A., Bump, J. K., Kang, S., & Klein, J. A. (2013). Climate change and water use partitioning by different plant functional groups in a grassland on the Tibetan plateau. *PLoS One*, 8(9), e75503. <https://doi.org/10.1371/journal.pone.0075503>

Johnson, J. E., Hamann, L., Dettman, D. L., Kim-Hak, D., Leavitt, S. W., Monson, R. K., & Papuga, S. A. (2017). Performance of induction module cavity ring-down spectroscopy (IM-CRDS) for measuring δ¹⁸O and δ²H values of soil, stem, and leaf waters. *Rapid Communications in Mass Spectrometry*, 31(6), 547–560. <https://doi.org/10.1002/rcm.7813>

Kerhouel, L. P., Kolb, T. E., & Koch, G. W. (2013). Tree size, stand density, and the source of water used across seasons by ponderosa pine in northern Arizona. *Forest Ecology and Management*, 289, 425–433. <https://doi.org/10.1016/j.foreco.2012.10.036>

Knapp, A. K., Fay, P. A., Blair, J. M., Collins, S. L., Smith, M. D., Carlisle, J. D., et al. (2002). Rainfall variability, carbon cycling, and plant species diversity in a Mesic grassland. *Science Reports*, 298(December), 2202–2205. <https://doi.org/10.1126/science.1076347>

Knowles, J. F., Scott, R. L., Biederman, J. A., Blanken, P. D., Burns, S. P., Dore, S., et al. (2020). Montane forest productivity across a semiarid climatic gradient. *Global Change Biology*, 26(12), 6945–6958. <https://doi.org/10.1111/gcb.15335>

Knowles, N., Dettinger, M. D., & Cayan, D. R. (2006). Trends in snowfall versus rainfall in the western United States. *Journal of Climate*, 19(18), 4545–4559. <https://doi.org/10.1175/JCLI3850.1>

Kumar, S., Newman, M., Wang, Y., & Livneh, B. (2019). Potential reemergence of seasonal soil moisture anomalies in North America. *Journal of Climate*, 32(10), 2707–2734. <https://doi.org/10.1175/JCLI-D-18-0540.1>

Kurpius, M. R., Panek, J. A., Nikolov, N. T., McKay, M., & Goldstein, A. H. (2003). Partitioning of water flux in a Sierra Nevada ponderosa pine plantation. *Agricultural and Forest Meteorology*, 117(3–4), 173–192. [https://doi.org/10.1016/S0168-1923\(03\)00062-5](https://doi.org/10.1016/S0168-1923(03)00062-5)

Kuznetsova, A., Brockhoff, P. B., & Christensen, R. H. B. (2017). lmerTest package: Tests in linear mixed effects models. *Journal of Statistical Software*, 82(13), 1–26. <https://doi.org/10.18637/jss.v082.i13>

Lenth, R. (2022). emmeans: Estimated Marginal Means, aka Least-Squares Means. R package version 1.8.2. Retrieved from <https://CRAN.R-project.org/package=emmeans>

Marshall, J. D., & Monserud, R. A. (2006). Co-occurring species differ in tree-ring δ¹⁸O trends. *Tree Physiology*, 26(8), 1055–1066. <https://doi.org/10.1093/treephys/26.8.1055>

Martin, J., Looker, N., Hoylman, Z., Jencso, K., & Hu, J. (2018). Differential use of winter precipitation by upper and lower elevation Douglas fir in the Northern Rockies. *Global Change Biology*, 24(12), 5607–5621. <https://doi.org/10.1111/gcb.14435>

McCormack, M. L., & Guo, D. (2014). Impacts of environmental factors on fine root lifespan. *Frontiers in Plant Science*, 5(May), 1–11. <https://doi.org/10.3389/fpls.2014.00205>

McDowell, N. G., Sapes, G., Pivovaroff, A., Adams, H. D., Allen, C. D., Anderegg, W. R. L., et al. (2022). Mechanisms of woody-plant mortality under rising drought, CO₂ and vapour pressure deficit. *Nature Reviews Earth & Environment*, 3(5), 294–308. <https://doi.org/10.1038/s43017-022-00272-1>

McNamara, J. P., Chandler, D., Seyfried, M., & Achet, S. (2005). Soil moisture states, lateral flow, and streamflow generation in a semi-arid, snowmelt-driven catchment. *Hydrological Processes*, 19(20), 4023–4038. <https://doi.org/10.1002/hyp.5869>

Nehemy, M. F., Maillet, J., Perron, N., Pappas, C., Sonnenstag, O., Baltzer, J. L., et al. (2022). Snowmelt water use at transpiration onset: Phenology, isotope tracing, and tree water transit time. *Water Resources Research*, 58(9), 1–22. <https://doi.org/10.1029/2022WR032344>

Peltier, D. M. P., & Ogle, K. (2019). Legacies of La Niña: North American monsoon can rescue trees from winter drought. *Global Change Biology*, 25(1), 121–133. <https://doi.org/10.1111/gcb.14487>

PRISM Climate Group, Oregon State University. Retrieved from <https://prism.oregonstate.edu>

R Core Team. (2022). *R: A language and environment for statistical computing*. R Foundation for Statistical Computing. Retrieved from <https://www.R-project.org/>

Roden, J. S., & Ehleringer, J. R. (2007). Summer precipitation influences the stable oxygen and carbon isotopic composition of tree-ring cellulose in *Pinus ponderosa*. *Tree Physiology*, 27(4), 491–501. <https://doi.org/10.1093/treephys/27.4.491>

Rossi, C., & Nimmo, J. R. (1994). Modeling of soil water retention from saturation to oven dryness. *Water Resources*, 30(March), 701–708. <https://doi.org/10.1029/93wr03238>

Seager, R., Ting, M., Held, I., Kushnir, Y., Lu, J., Vecchi, G., et al. (2007). Model projections of an imminent transition to a more arid climate in southwestern north America. *Science*, 305(May), 1181–1184. <https://doi.org/10.1126/science.1139601>

Seager, R., & Vecchi, G. A. (2010). Greenhouse warming and the 21st century hydroclimate of southwestern North America. *Proceedings of the National Academy of Sciences of the United States of America*, 107(50), 21277–21282. <https://doi.org/10.1073/pnas.0910856107>

Smith, T. J., Menamara, J. P., Flores, A. N., Gribb, M. M., Aishlin, P. S., & Benner, S. G. (2011). Small soil storage capacity limits benefit of winter snowpack to upland vegetation. *Hydrological Processes*, 25(25), 3858–3865. <https://doi.org/10.1002/hyp.8340>

Strange, B. M., Monson, R. K., Szejner, P., Ehleringer, J., & Hu, J. (2023). The North American Monsoon buffers forests against the ongoing megadrought in the Southwestern United States. *Global Change Biology*, 29(April), 4354–4367. <https://doi.org/10.1111/gcb.16762>

Szejner, P., Wright, W. E., Babst, F., Belmecheri, S., Troutet, V., Leavitt, S. W., et al. (2016). Latitudinal gradients in tree ring stable carbon and oxygen isotopes reveal differential climate influences of the North American Monsoon System. Received. <https://doi.org/10.1002/2016JG003460>

Szejner, P., Wright, W. E., Belmecheri, S., Meko, D., Leavitt, S. W., Ehleringer, J. R., & Monson, R. K. (2018). Disentangling seasonal and interannual legacies from inferred patterns of forest water and carbon cycling using tree-ring stable isotopes. *Global Change Biology*, 24(11), 5332–5347. <https://doi.org/10.1111/gcb.14395>

Tang, K., & Feng, X. (2001). The effect of soil hydrology on the oxygen and hydrogen isotopic compositions of plants' source water. *Earth and Planetary Science Letters*, 185(3–4), 355–367. [https://doi.org/10.1016/S0012-821X\(00\)00385-X](https://doi.org/10.1016/S0012-821X(00)00385-X)

Thomas, C. K., Law, B. E., Irvine, J., Martin, J. G., Pettijohn, J. C., & Davis, K. J. (2009). Seasonal hydrology explains interannual and seasonal variation in carbon and water exchange in a semiarid mature ponderosa pine forest in central Oregon. *Journal of Geophysical Research*, 114(4), 1–22. <https://doi.org/10.1029/2009JG001010>

Tulley-Cordova, C. L., Putman, A. L., & Bowen, G. J. (2021). Stable isotopes in precipitation and meteoric water: Sourcing and tracing the North American monsoon in Arizona, New Mexico, and Utah. *Water Resources Research*, 57(12), 1–18. <https://doi.org/10.1029/2021WR030039>

Urrutia-Jalabert, R., Barichivich, J., Szejner, P., Rozas, V., & Lara, A. (2023). Ecophysiological responses of *Nothofagus obliqua* forests to recent climate drying across the Mediterranean-temperate biome transition in south-Central Chile. *Journal of Geophysical Research: Biogeosciences*, 128(4), 1–18. <https://doi.org/10.1029/2022JG007293>

USDA Natural Resources Conservation Service. (2022). *SNOWpack TELEmetry Network (SNOWTEL)*. NRCS. Retrieved from <https://data.nal.usda.gov/dataset/snowpack-telemetry-network-snotel>

West, A. G., Goldsmith, G. R., Brooks, P. D., & Dawson, T. E. (2010). Discrepancies between isotope ratio infrared spectroscopy and isotope ratio mass spectrometry for the stable isotope analysis of plant and soil waters. *Rapid Communications in Mass Spectrometry*, 24(14), 1948–1954. <https://doi.org/10.1002/rcm>

Westerling, A., Hidalgo, H., Cayan, D., & Swetnam, T. (2006). Warming and earlier spring increase western U.S. Forest wildfire activity. *Science*, 313(August), 940–943. <https://doi.org/10.1126/science.1128834>

Williams, A. P., Cook, B. I., & Smerdon, J. E. (2022). Rapid intensification of the emerging southwestern North American megadrought in 2020–2021. *Nature Climate Change*, 12(3), 232–234. <https://doi.org/10.1038/s41558-022-01290-z>

Williams, A. P., Cook, E. R., Smerdon, J. E., Cook, B. I., Abatzoglou, J. T., Bolles, K., et al. (2020). Large contribution from anthropogenic warming to an emerging North American megadrought. *Science*, 370(6516), 314–318. <https://doi.org/10.1126/SCIENCE.ABF3676>